

# Efficient Path Planning and Task Allocation Algorithm for Boolean Specifications

Ioana Hustiu, Roozbeh Abolpour, Marius Kloetzer and Cristian Mahulea, *Senior Member, IEEE*

**Abstract**—This paper addresses path planning and task allocation in multi-robot systems subject to global Boolean specifications defined on the final state. The main contribution is the exploitation of the structural properties of a Petri net model of robot motion: we prove that the associated constraint matrix is *totally unimodular* (TU). This property allows relaxing the original Integer Linear Programming (ILP) formulation to a Mixed Integer Linear Programming (MILP) in which all variables are continuous except for a small set of integer variables, whose number equals the atomic propositions in the Boolean specification. This yields a substantial reduction in complexity. In the special case where the specification is a conjunction of atomic propositions of cardinality equal to the team size, i.e., the standard Task-Assignment and Path Finding (TAPF) problem, the formulation reduces entirely to a Linear Programming (LP). Collision-free paths are ensured by introducing intermediate synchronization points only when necessary, while robots move in parallel between them. These structural insights enable a computationally efficient solution for large-scale problems with up to 2500 robots, ensuring both tractability and safety in multi-robot coordination.

**Index Terms**—mobile robots, path planning, Petri nets, task assignment

## I. INTRODUCTION

**P**ATH planning for mobile robots is a fundamental problem in robotics, with applications ranging from industrial automation to autonomous exploration. As some approaches are based on graph search planning techniques [1], [2], others aim to achieve scalability by combining sequential planning with time-optimal and collision-free trajectories [3] or include heuristic methods in the solution [4], [5]. In general, such problems of finding path(s) for each robot are requiring to coordinate multiple agents in a shared environment, which can become a sophisticated challenge.

Research has shown that MILP formulations are powerful tools for encoding different types of constraints due to their flexibility in a unified mathematical framework [6], [7]. Applications of MILP in multi-robot path planning have showed the

This work was supported in part by grant PID2024-159284NB-I00 funded by MCIN/AEI/10.13039/501100011033 and by the “European Union NextGenerationEU/PRTR” and by Grant N62909-24-1-2081 funded by Office of Naval Research Global, USA. (Corresponding author: Ioana Hustiu)

Ioana Hustiu and Marius Kloetzer are with the Department of Automatic Control and Applied Informatics, Technical University “Gheorghe Asachi” of Iasi, 700050 Iasi, Romania (e-mail: ioana.hustiu@academic.tuiasi.ro; marius.kloetzer@academic.tuiasi.ro).

Roozbeh Abolpour is with the Energy Information Networks and Systems Group at the Technical University of Darmstadt, 64289 Darmstadt, Germany (e-mail: roozbeh.abolpour@eins.tu-darmstadt.de).

Cristian Mahulea is with the Aragón Institute for Engineering Research (I3A), University of Zaragoza, 50018 Zaragoza, Spain (email: cmahulea@unizar.es).

ability to handle multiple constraints such as obstacle avoidance and task allocation [8]. However, their computational complexity, being NP-hard, limits the scalability for large robotic systems, motivating the need to explore alternative techniques [9]. It is known that MILP solvers are providing a solution in reasonable time only for relatively small problems and tend to not be scalable w.r.t. the size of the problem. Thus, various heuristic algorithms have been proposed to compute near-optimal solutions [6], next to suboptimal iterative searches [10] or branch-and-Benders-cut schemes [11].

A common approach to manage the complexity of multi-robot path planning has been to leverage formal models such as Boolean or Temporal Logic and Petri nets (PN) to specify task constraints [12], [13]. For example, Petri nets can be integrated with LTL specifications into a composed Petri net to provide collision-free trajectories with an attractive computational time [14] or can be used in modelling critical application features of a robotic team through a set of complex coordination rules [15]. By being able to provide effective solutions for systems that require complex tasks and logical dependencies, Petri nets are a natural fit in multi-robot systems topic [16].

Motivated by the aforementioned context, this paper addresses the task allocation and collision-free path planning problem with Boolean task specification on the final team state, utilizing Petri net models. The solution builds on the ILP and MILP formulations introduced in [17] and [18]. The technical contributions are stated at the end of Section II.

## II. RELATED WORK AND CONTRIBUTIONS

Multi-Agent Path Finding (MAPF) is the problem of computing collision-free paths for a team of agents moving in a shared environment while using given pairs of start-goal locations. If the goals are not already assigned to the mobile robots, then the task allocation must also be performed and this formulation is called Task-Assignment and Path Finding (TAPF) [19]. This paper is closely aligned with the second framework, while both are extensively studied [20]–[23].

Task-Assignment (TA) is a challenge in multi-robot systems, and the literature reflects a wide spectrum of solutions for it. Graph-based formulations are one of the most used paradigms, where the TA is tightly integrated with path planning through the construction of conflict search trees [24], [25]. Alternative perspectives include auction methods [26], [27], rule-based solutions [28] and heuristic approaches, but in many cases, they sacrifice optimality for efficiency [29], [30]. Our work adopts another common strategy, namely the optimization paradigm, but extends the TAPF problem by integrating task

allocation for fulfilling a Boolean specification, instead of fixed goals. These optimization-based approaches may have scalability issues [31], [32], but we manage to overcome this challenge, demonstrating efficiency and scalability with teams of up to 2500 robots by exploiting the unimodularity property of the constraint matrix and avoid solving an ILP formulation. To better contextualize our contribution in this direction, we will later compare our framework with several representative methods from the literature. This comparison not only highlights the advantages of our approach but also better positions it within the literature.

With respect to the path planning aspect, i.e., MAPF problem, one of the most established solutions that are making use of graphs is the Conflict-Based Search (CBS) [20]. However, recent works have explored alternatives to integrate a learning component to better handle complex environments [33], [34]. A different solution using a hybrid policy that switches between a reinforcement learning (RL) approach and a heuristic search for a partially observable environment has also been addressed in recent literature [35], but it may not exhibit strong scalability or high effectiveness in handling collision avoidance [36]. Work [37] is proposing a combination between Petri nets and RL for solving the path planning problem for a team of automated guided vehicles. In order to avoid collision, place timed Petri nets are used and deadlocks may appear, together with transition loops. Our method, on the other hand, explicitly enforces collision avoidance using constraints, while guaranteeing the absence of such transition loops by minimizing the number of movements of the robots.

The main contribution of this paper lies in exploiting the structural properties of the constraint matrix derived from the Petri net model. We formally prove that this matrix is *totally unimodular (TU)*, which enables the relaxation of the original ILP formulation into a linear program without compromising the integrality or optimality of the solution. This relaxation eliminates the need for combinatorial search procedures, significantly improving scalability and computational efficiency in multi-robot path planning. Building upon this result, we extend the classical TAPF formulation to handle *Boolean specifications*, allowing the automatic selection of the tasks to be fulfilled in the robots' final state. The proposed algorithm demonstrates strong scalability—successfully coordinating teams of up to **2500 robots**—and includes rigorous mathematical proofs that consolidate its theoretical foundation. Extensive simulations on standard benchmark maps confirm both the efficiency and robustness of the approach compared to existing methods, highlighting its relevance for complex, large-scale multi-robot coordination problems.

### III. PROBLEM DEFINITION

Consider a team of  $n_R$  identical mobile robots operating in a known and static environment, where disjoint regions of interest are dispersed. The environment is divided into a finite set of cells, denoted by  $P = \{p_1, \dots, p_{|P|}\}$ , using a region-preserving cell decomposition method [38], [39]. We assume that  $\mathcal{Y} = \{y_1, \dots, y_{|\mathcal{Y}|}\}$  is a set of atomic propositions used to label the regions of interest. The correlation between cells and

regions is ensured by a labeling function  $h : P \rightarrow \mathcal{Y} \cup \{\emptyset\}$ , i.e.,  $h(p_i)$  associates a cell  $p_i$  with a region of interest, while  $h(p_i) = \emptyset$  indicates that  $p_i$  lies in the free space.

To model the movement of the robots within the environment, the Robot Motion Petri Net (RMPN) is used [39].

**Definition 1.** A Robot Motion Petri net (RMPN) system is defined as a tuple  $\Sigma_N = \langle \mathcal{N}, \mathbf{m}_0, \mathcal{Y}, h \rangle$ , where:

- $\mathcal{N} = \langle P, T, \mathbf{Pre}, \mathbf{Post} \rangle$  is a Petri net, with  $P$  the set of places and  $T$  the set of transitions. The pre-incidence matrix  $\mathbf{Pre} \in \{0, 1\}^{|P| \times |T|}$  and the post-incidence matrix  $\mathbf{Post} \in \{0, 1\}^{|P| \times |T|}$  define the arcs from places towards transitions and from transitions towards places.
- $\mathbf{m}_0 \in \mathbb{N}_{\geq 0}^{|P|}$  is the initial marking, where  $\mathbf{m}_0[p_i]$  gives the number of robots located in place  $p_i$  at the initial state.
- $h : P \rightarrow \mathcal{Y} \cup \{\emptyset\}$  is the labeling function defined over the set of possible symbols that a mobile robot can observe.

An RMPN is a subclass of Petri nets, specifically a *state machine*, as each transition has by definition exactly one input and one output place [39]. In this model, each robot is represented by a token and thus the model maintains its topology for different team sizes.

We define the matrix  $\mathbf{V} \in \{0, 1\}^{|\mathcal{Y}| \times |P|}$  such that  $\mathbf{V}[i, j] = 1$  if  $h(p_j) = y_i$ , and  $\mathbf{V}[i, j] = 0$  otherwise. Furthermore, let  $\mathbf{C} = \mathbf{Post} - \mathbf{Pre}$  denote the token flow matrix, which describes the effect of firing any transition  $t_j \in T$ . Firing an enabled transition  $t_j$  consumes a token from its input place ( $\bullet t_j$ ) and produces a token at its output place ( $t_j \bullet$ ), representing the movement of a robot between adjacent cells.

If a sequence of transitions is fired, the vector  $\boldsymbol{\sigma}$ , known as the firing count vector, represents the number of times each transition is fired. The initial marking  $\mathbf{m}_0$  changes as transitions fire, and the obtained final marking  $\mathbf{m}_f$  is determined by the PN state equation:

$$\mathbf{m}_f = \mathbf{m}_0 + \mathbf{C} \cdot \boldsymbol{\sigma} \quad (1)$$

**Example 1.** Consider an environment with 4 cells  $\{p_1, p_2, p_3, p_4\}$ , 2 regions of interest  $\{y_1, y_2\}$  and a single mobile robot that is placed in cell  $p_3$ . Fig. 1 illustrates the RMPN system that describes this environment and consists of  $P = \{p_1, p_2, p_3, p_4\}$ ,  $T = \{t_1, \dots, t_8\}$  and the initial marking  $\mathbf{m}_0 = [0, 0, 1, 0]^T$ . The incidence matrix for the RMPN is:

$$\mathbf{C} = \begin{matrix} & t_1 & t_2 & t_3 & t_4 & t_5 & t_6 & t_7 & t_8 \\ \begin{matrix} p_1 \\ p_2 \\ p_3 \\ p_4 \end{matrix} & \begin{bmatrix} -1 & 1 & 0 & 0 & 0 & 0 & 1 & -1 \\ 1 & -1 & -1 & 1 & -1 & 1 & 0 & 0 \\ 0 & 0 & 1 & -1 & 0 & 0 & 0 & 0 \\ 0 & 0 & 0 & 0 & 1 & -1 & -1 & 1 \end{bmatrix} \end{matrix}.$$

Each column of the incidence matrix  $\mathbf{C}$  represents the effect of firing a transition. Here, the transition  $t_1$  models the movement of a robot from cell  $p_1$  to cell  $p_2$ . Moreover, we have  $h(p_1) = \{y_2\}$ ,  $h(p_2) = \emptyset$ ,  $h(p_3) = \emptyset$  and  $h(p_4) = \{y_1\}$ . Hence, the

characteristic matrix is  $\mathbf{V} = \begin{matrix} & p_1 & p_2 & p_3 & p_4 \\ \begin{matrix} y_1 \\ y_2 \end{matrix} & \begin{bmatrix} 0 & 0 & 0 & 1 \\ 1 & 0 & 0 & 0 \end{bmatrix} \end{matrix}$ . We have  $\mathbf{V} \cdot \mathbf{m}_0 = [0, 0]^T$  meaning that in its current position

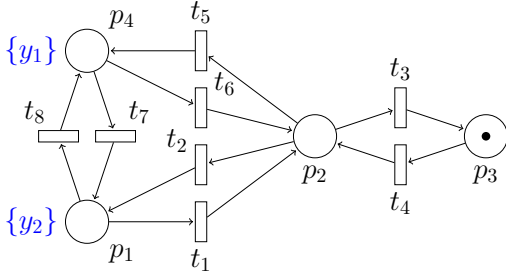


Fig. 1: Example of a RMPN.

$m_0$ , the mobile agent is not observing  $y_1$ , nor  $y_2$  (the token is placed in  $p_3$  which represents the free space).

Assume that  $t_4$  and  $t_2$  will be fired, the firing count vector will be  $\sigma = [0, 1, 0, 1, 0, 0, 0, 0]^T$ . According to (1), the final marking will be  $m_f = [1, 0, 0, 0]^T$  and when computing  $V \cdot m_f$  we obtain  $[1, 0]^T$ , which means that our agent is observing the region labelled with  $y_2$ , since  $h(p_1) = \{y_2\}$ . ■

**Problem 1.** Given a team of  $n_R$  mobile robots and a Boolean formula  $\varphi$  defined over the set of atomic propositions  $\mathcal{Y}$  find collision-free paths for the mobile robots to reach a final state (marking) at which the global Boolean-based specification  $\varphi$  is fulfilled.

Please note that Problem 1 is an extension of the classical TAPF formulation by imposing to satisfy the Boolean goal in the final state of the robotic team. This means that we do not have knowledge of what those tasks from the set  $\mathcal{Y}$  will be assigned to robots. In this work, a trajectory (or path) denotes the sequence of cells a robot follows from its start to its destination. The Boolean formula  $\varphi$ , representing a global task, specifies regions to be visited or avoided, thereby defining task completion and requiring robot-to-task allocations. We assume the goal is feasible, i.e., a final state (marking) exists at which  $\varphi$  is satisfied. Cases where more regions than available robots must be visited are not considered in this framework. Without loss of generality, let  $\varphi = \varphi_1 \wedge \dots \wedge \varphi_{n_d}$  be in Conjunctive Normal Form (CNF), where each term  $\varphi_i$  is a disjunction of literals from  $\mathcal{Y}$ . Following the approach described in [40], we convert  $\varphi$  into linear inequalities. To represent the regions visited at the final marking, we introduce a binary vector  $\mathbf{x} \in \{0, 1\}^{|\mathcal{Y}|}$ , where  $x_i = 1$  if region  $y_i$  is visited, and  $x_i = 0$  otherwise. The linear constraints corresponding to the formula  $\varphi$  can be written as:  $A_\varphi \cdot \mathbf{x} \leq \mathbf{b}_\varphi$ , where  $A_\varphi \in \{-1, 0, 1\}^{n_d \times |\mathcal{Y}|}$  and  $\mathbf{b}_\varphi \in \mathbb{N}_{\geq 0}^{n_d}$ . Here,  $n_d$  is the number of conjunctions from the CNF of  $\varphi$ . The entries of  $A_\varphi$  are defined as follows:

$$A_\varphi[i, j] = \begin{cases} -1, & \text{if } y_j \text{ appears positively in } \varphi_i, \\ 1, & \text{if } \neg y_j \text{ appears in } \varphi_i, \\ 0, & \text{otherwise.} \end{cases} \quad (2)$$

where each of the  $i^{\text{th}}$  elements of vector  $\mathbf{b}_\varphi$  corresponds to the  $i^{\text{th}}$  term found in conjunction (in the CNF form) and

indicates the numbers of negated literals (not observed) minus one as explained in [40].

**Example 2.** Consider the Boolean formula defined over  $\mathcal{Y} = \{y_1, y_2, y_3, y_4\}$ :

$$\varphi = (y_1 \vee y_2 \vee y_4) \wedge (\neg y_2 \vee y_3 \vee y_4) \wedge (\neg y_1 \vee y_3).$$

According to (2),  $\varphi$  translates to:

$$A_\varphi = \begin{bmatrix} -1 & -1 & 0 & -1 \\ 0 & 1 & -1 & -1 \\ 1 & 0 & -1 & 0 \end{bmatrix} \quad \text{and} \quad \mathbf{b}_\varphi = \begin{bmatrix} -1 \\ 0 \\ 0 \end{bmatrix}. \blacksquare$$

**Collision Avoidance.** To guarantee collision-free paths, we can impose that each cell  $p_i$  is crossed by at most one robot when moving from the initial marking  $m_0$  to the final marking  $m_f$ . This strict condition can be written as:

$$\mathbf{Post} \cdot \sigma + m_0 \leq \mathbf{1}. \quad (3)$$

While conservative, this condition guarantees parallel free movements from  $m_0$  to  $m_f$  without synchronization.

In many practical cases, however, condition (3) may be too restrictive. For example, when a narrow passage, e.g., a bridge, must be crossed by several robots to reach their destinations. To handle such cases, we introduce an auxiliary variable  $s$  that represents the maximum number of robots allowed to occupy the same region simultaneously:

$$\mathbf{Post} \cdot \sigma + m_0 \leq s \cdot \mathbf{1}. \quad (4)$$

The minimum value of  $s$  satisfying (4) corresponds to the infinite norm  $s = \|\mathbf{Post} \cdot \sigma + m_0\|_\infty$ , i.e., the maximum number of robots crossing any region along paths. In the optimization problem,  $s$  is minimized with a large weight in the cost function, forcing solutions with minimal congestion.

If the optimal solution<sup>1</sup> yields  $s^* = 1$ , then fully parallel, collision-free trajectories are obtained directly. Otherwise, if  $s^* > 1$ , we introduce  $\lceil s^* \rceil$  intermediate markings, which act as synchronization points ensuring that at most one enters a region at a time. Unlike the solution in [12], which relies on assigning priorities, in this paper we explicitly construct such intermediate markings. In some situations, introducing exactly  $\lceil s^* \rceil$  synchronizations may still be insufficient due to multiple interconnected narrow passages. In practice, however, this is rare, and feasibility can usually be obtained by incrementing the number of intermediate markings by one. In our simulations, one or two such increments were always sufficient to obtain a feasible, collision-free solution. Between two consecutive synchronizations, robots again move in parallel.

The complete robot path planning problem for the extended TAPF can now be formulated as follows [17]:

<sup>1</sup>Through the paper, the symbol  $*$  indicates the optimal solution.

$$\begin{aligned}
& \text{Minimize} && \mathbf{1}^T \cdot \boldsymbol{\sigma} + M \cdot s \\
& \text{Subject to:} && \mathbf{m} = \mathbf{m}_0 + \mathbf{C} \cdot \boldsymbol{\sigma}, & (a) \\
& && \mathbf{x} \leq \mathbf{V} \cdot \mathbf{m} \leq N \cdot \mathbf{x}, & (b) \\
& && \mathbf{A}_\varphi \cdot \mathbf{x} \leq \mathbf{b}_\varphi, & (c) \\
& && \mathbf{Post} \cdot \boldsymbol{\sigma} + \mathbf{m}_0 \leq s \cdot \mathbf{1}^{|\mathcal{P}|}, & (d) \\
& && \mathbf{m} \geq \mathbf{0}^{|\mathcal{P}|}, \boldsymbol{\sigma} \geq \mathbf{0}^{|\mathcal{T}|}, & (e) \\
& && \mathbf{0}^{|\mathcal{Y}|} \leq \mathbf{x} \leq \mathbf{1}^{|\mathcal{Y}|}, s \geq 1.
\end{aligned} \tag{5}$$

In (5), the unknowns are represented by the tuple  $(\mathbf{m}, \boldsymbol{\sigma}, \mathbf{x}, s)$ , while  $N > n_R + 1$  and  $M > |\mathcal{T}| + 1$  are sufficiently large positive constants used to force feasibility and prioritize collision avoidance. We will report only the first term of the cost function, as the second term serves only as an auxiliary factor in the optimization and not as a performance metric. The constraints have the following meaning: (a) is the state equation (1), linking the initial marking  $\mathbf{m}_0$ , the final marking  $\mathbf{m}$ , the incidence matrix  $\mathbf{C}$ , and the firing vector  $\boldsymbol{\sigma}$ ; (b) relates the final marking  $\mathbf{m}$  with the Boolean variables  $\mathbf{x}$ , using the labelling matrix  $\mathbf{V}$ ; (c) encodes the global Boolean specification on the final state; (d) limits the number of robots that can simultaneously occupy a cell to  $s$ . This variable  $s$  captures the maximum congestion along the path and (e) enforces boundary conditions for the unknowns.

**Remark 1.** *Since our approach relies on LP relaxations, we will denote the problem type as (5) – (.). Specifically, (5) – ILP uses only integer variables, (5) – MILP treats most of the variables as continuous while keeping a subset as integer, and (5) – LP relaxes all variables to be continuous.*

**Remark 2.** *While the ILP approach in [17] may exhibit slow performance when the number of integer variables is high, our method addresses this limitation by leveraging a mathematical framework inspired by the LP relaxation. This will allow us to reach great scalability, while computing efficiently the optimal solution w.r.t. the number of firings.*

#### IV. UNIMODULAR AND TOTALLY UNIMODULAR MATRICES

In integer programming, one of the key challenges is that solving an ILP problem is, in general, NP-hard. In our context, this difficulty appears naturally when encoding robot motion and Boolean specifications as ILPs. However, there exist structural properties of the constraint matrix that guarantee that the relaxation to Linear Programming (LP) already produces integer solutions with a lower complexity [41]. This is exactly the role of unimodular and totally unimodular (TU) matrices.

A *unimodular matrix* is a square integer matrix  $\mathbf{S}$  with determinant equal to  $\pm 1$ . Equivalently,  $\mathbf{S}$  is invertible over the integers, i.e., there exists another integer matrix  $\mathbf{S}'$  such that  $\mathbf{S} \cdot \mathbf{S}' = \mathbf{S}' \cdot \mathbf{S} = \mathbf{I}$ . As a direct consequence, for any integer vector  $\mathbf{b}$ , the system  $\mathbf{S} \cdot \mathbf{x} = \mathbf{b}$  has an integer solution. Classical examples of unimodular matrices include the identity matrix, its negative, the inverse of a unimodular matrix, or the product of two unimodular matrices [41].

The concept of *total unimodularity* generalizes unimodularity from a single square matrix to all square submatrices of a given rectangular one.

**Definition 2.** *A matrix  $\mathbf{A} \in \mathbb{Z}^{m \times n}$  is totally unimodular (TU) if every square submatrix has the determinant 0 or  $\pm 1$ .*

This property has profound implications in optimization. The following theorem is central [41]:

**Theorem 1.** *Let  $\mathbf{A} \in \mathbb{Z}^{m \times n}$  be totally unimodular and let  $\mathbf{b} \in \mathbb{Z}^m$  be an integer right-hand side vector. Then every vertex (extreme point) of the polyhedron*

$$\{\mathbf{x} \in \mathbb{R}_{\geq 0}^n \mid \mathbf{A} \cdot \mathbf{x} \leq \mathbf{b}\}$$

*is integer. Consequently, the LP relaxation of any integer program with constraint matrix  $\mathbf{A}$  and integral  $\mathbf{b}$  admits an integer optimal solution.*

The relevance of TU matrices is that they allow replacing computationally intractable ILPs with tractable LPs without losing integrality. This avoids the need for branch-and-bound or cutting-plane techniques, as the LP solver directly returns integer solutions. In practice, many combinatorial optimization problems admit formulations with TU matrices. For example, bipartite matching, network flows, and circulation problems all rely on TU structures, which explains why they are solvable efficiently using LP methods.

Several equivalent characterizations exist for total unimodularity, among which we use Ghouila-Houri's [41].

**Theorem 2.** *A matrix  $\mathbf{A} \in \mathbb{R}^{m \times n}$  is totally unimodular if and only if, for every subset of rows  $R \subseteq \{1, \dots, m\}$ , there exists a partition  $R = R_1 \cup R_2$  such that for every  $j \in \{1, \dots, n\}$  (column index),*

$$\sum_{i \in R_1} A_{ij} - \sum_{i \in R_2} A_{ij} \in \{-1, 0, 1\}.$$

As shown in the following sections, the constraint matrices derived from the RMPN and TAPF formulations are TU. This property guarantees that the LP relaxations, when solved using a simplex-based algorithm, yield integer solutions.

#### V. TASK-ASSIGNMENT AND PATH FINDING PROBLEM

In this section, we show that the classical Task-Assignment and Path Finding (TAPF) problem can be expressed as a special case of our framework with Boolean specifications. Specifically, consider a global specification defined over  $|\mathcal{Y}|$  disjoint regions of interest, with  $|\mathcal{Y}| = n_R$ . The Boolean specification is a conjunction of all regions, i.e.,  $\varphi = y_1 \wedge y_2 \wedge \dots \wedge y_{|\mathcal{Y}|}$ .

This requires that every region is occupied in the final state. Hence, the vector  $\mathbf{x}^*$ , solution of (5), should have all entries equal to 1. In this setting, we deal with both task allocation and path planning problems: robots must distribute themselves among the regions while minimizing the total travelled distance. The final marking is uniquely determined as  $\mathbf{m}_f = \mathbf{V}^T \cdot \mathbf{x}$ , with  $\mathbf{x} = \mathbf{1}^{|\mathcal{Y}|}$ .

Thus, the general optimization problem (5) simplifies considerably. Since the final marking is known, only constraints (a), (d) and (e) are retained, yielding the reduced formulation.

$$\begin{aligned}
& \text{Minimize} && \mathbf{1}^T \cdot \boldsymbol{\sigma} + N \cdot s \\
& \text{Subject to:} && \mathbf{C} \cdot \boldsymbol{\sigma} = \mathbf{m}_f - \mathbf{m}_0, & (a) \\
& && \mathbf{Post} \cdot \boldsymbol{\sigma} + \mathbf{m}_0 \leq s \cdot \mathbf{1}, & (b) \\
& && \boldsymbol{\sigma} \geq \mathbf{0}^{|\mathcal{T}|}, s \geq 0. & (c)
\end{aligned} \tag{6}$$

The unknowns in (6) are the firing vector  $\boldsymbol{\sigma}$  and the scalar  $s$ . Problem (5) therefore captures the general case with arbitrary Boolean specifications and implicit task allocation, while (6) corresponds exactly to the TAPF setting, where the specification is the conjunction of all  $|\mathcal{Y}|$  regions and the destinations are fully determined.

For problem (6) - LP (that is,  $\boldsymbol{\sigma} \in \mathbb{R}_{\geq 0}^{|\mathcal{T}|}$  and  $s \in \mathbb{R}_{\geq 0}$ ), if the optimal solution  $s^*$  is integer, then  $\boldsymbol{\sigma}^*$  is also integer. This follows because, when  $s$  is fixed to an integer value, the constraint matrix of (6) reduces to the one analysed in Theorem 3, which is totally unimodular. Hence, the LP relaxation already guarantees integrality of  $\boldsymbol{\sigma}$  under this condition.

**Theorem 3.** *In a state machine Petri net, the vertical concatenation of  $\mathbf{C}$  and  $\mathbf{Post}$  matrices, i.e.,  $\begin{bmatrix} \mathbf{C} \\ \mathbf{Post} \end{bmatrix}$ , is TU.*

*Proof.* The formal proof is available in the appendix A.  $\square$

**Example 3.** *Recall the RMPN model described in Ex. 1. The constraint matrix constructed as explained at the beginning of this section is:*

$$\begin{aligned}
& \text{this section is: } \begin{bmatrix} \mathbf{C} \\ \mathbf{Post} \end{bmatrix} = \\
& \begin{array}{l} 1: p_1 \\ 2: p_2 \\ 3: p_3 \\ 4: p_4 \\ 5: p_1 \\ 6: p_2 \\ 7: p_3 \\ 8: p_4 \end{array} \begin{array}{c} t_1 \quad t_2 \quad t_3 \quad t_4 \quad t_5 \quad t_6 \quad t_7 \quad t_8 \\ \left[ \begin{array}{cccccccc} -1 & 1 & 0 & 0 & 0 & 0 & 1 & -1 \\ 1 & -1 & -1 & 1 & -1 & 1 & 0 & 0 \\ 0 & 0 & 1 & -1 & 0 & 0 & 0 & 0 \\ 0 & 0 & 0 & 0 & 1 & -1 & -1 & 1 \\ \dots & \dots \\ 0 & 1 & 0 & 0 & 0 & 0 & 1 & 0 \\ 1 & 0 & 0 & 1 & 0 & 1 & 0 & 0 \\ 0 & 0 & 1 & 0 & 0 & 0 & 0 & 0 \\ 0 & 0 & 0 & 0 & 1 & 0 & 0 & 1 \end{array} \right] \end{array}
\end{aligned}$$

We arbitrarily select the sub-matrix with  $R = \{1, 3, 4, 5, 6\}$ , i.e., rows corresponding to  $p_1, p_3$  and  $p_4$  from  $\mathbf{C}$  and rows corresponding to  $p_1$  and  $p_2$  from  $\mathbf{Post}$ .

Based on the proof of Theorem 1, all the rows of  $\mathbf{C}$  will be placed in partition  $R_1$ , meaning that we will have  $R_1 = \{1, 3, 4\}$ . The summation on columns will be equal with -1 for column 1, 1 for column 2 and so on. When evaluating the rows of matrix  $\mathbf{Post}$ , we have that row 5 corresponds to row 1 from  $\mathbf{C}$  and will be included in  $R_2$ , while row 6 does not have a correspondent in  $\mathbf{C}$  and will be included in  $R_1$ .

The final partitioning of the rows of  $R$  are as it follows:  $R_1 = \{1, 3, 4, 6\}$  and  $R_2 = \{5\}$  with  $R = R_1 \cup R_2$ .  $\blacksquare$

After solving (6), if  $s^*$  is equal with 1, then collision-free trajectories are already obtained, while if  $s^* > 1$ , collisions are occurring. In this case, we will introduce a number of  $\bar{s} = \lceil s^* \rceil$  intermediate markings. This idea is can be translated in the following formulation, where the second term of the objective function is forcing the robotic movement in the first iterations:

$$\begin{aligned}
& \text{Minimize} && \mathbf{1}^T \cdot \boldsymbol{\sigma}_i \cdot \left( \sum_{i=1}^{\bar{s}} 1 + (\bar{s} - i) \right) \\
& \text{Subject to:} && \mathbf{m}_i = \mathbf{m}_{i-1} + \mathbf{C} \cdot \boldsymbol{\sigma}_i, i = 1, \dots, \bar{s} & (a) \\
& && \mathbf{Post} \cdot \boldsymbol{\sigma}_i + \mathbf{m}_{i-1} \leq \mathbf{1}, i = 1, \dots, \bar{s} & (b) \\
& && \mathbf{m}_{\bar{s}} = \mathbf{m}_f & (c) \\
& && \mathbf{m}_i \geq 0, i = 1, \dots, \bar{s} - 1, & (d_1) \\
& && \boldsymbol{\sigma}_i \geq 0, i = 1, \dots, \bar{s}, & (d_2)
\end{aligned} \tag{7}$$

Please note that the variables from problem (7) are the intermediate markings  $\mathbf{m}_i, i = 1, \dots, \bar{s}$  and their associated firing count vectors,  $\boldsymbol{\sigma}_i, i = 1, \dots, \bar{s}$ .

**Theorem 4.** *For a state machine Petri net, the matrix*

$$\begin{bmatrix} -\mathbf{I} & \mathbf{C} & \mathbf{0} & \mathbf{0} & \mathbf{0} & \mathbf{0} & \mathbf{0} & \vdots \\ \mathbf{0} & \mathbf{Post} & \mathbf{0} & \mathbf{0} & \mathbf{0} & \mathbf{0} & \mathbf{0} & \vdots \\ \mathbf{I} & \mathbf{0} & -\mathbf{I} & \mathbf{C} & \mathbf{0} & \mathbf{0} & \mathbf{0} & \vdots \\ \mathbf{I} & \mathbf{0} & \mathbf{0} & \mathbf{Post} & \mathbf{0} & \mathbf{0} & \mathbf{0} & \vdots \\ \mathbf{0} & \mathbf{0} & \mathbf{I} & \mathbf{0} & -\mathbf{I} & \mathbf{C} & \mathbf{0} & \vdots \\ \mathbf{0} & \mathbf{0} & \mathbf{I} & \mathbf{0} & \mathbf{0} & \mathbf{Post} & \mathbf{0} & \vdots \\ \dots & \dots \end{bmatrix}$$

is TU.

*Proof.* The proof follows the same approach as Theorem 3, applying a similar row partitioning as follows:

- Partition  $R_1$  contains all the rows that are corresponding to the incidence matrix  $\mathbf{C}$  for any intermediate marking.
- Partition  $R_2$  includes only those rows from  $\mathbf{Post}$  that do have a correspondent in paired matrix  $\mathbf{C}$  (the matrix  $\mathbf{C}$  of the above row).

Unlike Theorem 3, the difference lies in  $-\mathbf{I}$  and  $\mathbf{I}$  matrices, yielding column sums of  $-1, 0$  and  $1$ . Hence, the concatenation of the matrices  $-\mathbf{I}, \mathbf{I}, \mathbf{C}$  and  $\mathbf{Post}$ , in the manner described above, is TU.  $\square$

Solving (7) - LP with dual-simplex method will lead to an integer solution based on Theorem 4. If infeasible, the problem can be solved again with more intermediate markings. Even if the problem size grows with  $\bar{s}$ , the upper bound of the number of intermediate markings is equal to the team size when the final destinations are reached sequentially.

## VI. EXTENDED TAPF SOLUTION STRATEGY

We now return to the complete formulation (5), which includes the decision variable  $\mathbf{x}$ . The solution proceeds in two stages that combine the LP relaxation ideas of Section IV with the collision-avoidance mechanism described previously.

**Stage I: LP relaxation of (5).** We first solve (5)-LP, where all variables  $(\mathbf{m}, \boldsymbol{\sigma}, \mathbf{x}, s)$  are relaxed to be continuous.

- If the relaxation is infeasible, then the original ILP is also infeasible, since the LP enlarges the feasible region.

- Otherwise, let  $(\mathbf{m}^*, \boldsymbol{\sigma}^*, \mathbf{x}^*, s^*)$  be the optimal LP solution.

Two situations arise:

- 1) If  $s^* = 1$  and  $\mathbf{x}^*$  is integer, the solution is feasible and collision-free. In this case,  $\mathbf{m}^*$  and  $\boldsymbol{\sigma}^*$  are guaranteed to be integer. Indeed, once  $\mathbf{x}^*$  is integers, constraint (5)-(c) becomes redundant and (5)-(b) reduces to simple bounds on  $\mathbf{m}$  (since  $\mathbf{V}$  is a submatrix of the identity). The remaining constraint matrix can be written as

$$\begin{bmatrix} \mathbf{C} & -\mathbf{I} \\ \mathbf{Post} & \mathbf{0} \end{bmatrix}.$$

From Theorem 3, we know that the vertical concatenation  $\begin{bmatrix} \mathbf{C} \\ \mathbf{Post} \end{bmatrix}$  is TU. Appending the block  $\begin{bmatrix} -\mathbf{I} \\ \mathbf{0} \end{bmatrix}$  corresponds to concatenating this TU matrix with an identity matrix, an operation that preserves total unimodularity (see, e.g., [41]). Therefore, the full matrix above is also TU.

- 2) Otherwise (i.e., if  $s^* > 1$  or  $\mathbf{x}^*$  is fractional), we set the number of required synchronizations to  $\bar{s} = \lceil s^* \rceil$  and proceed to Stage II.

**Stage II: Collision-free refinement with intermediate markings.** In this stage,  $\mathbf{x}$  is explicitly kept as a binary decision variable, ensuring that the Boolean specification is satisfied exactly. We then construct the extended formulation (8), which introduces  $\bar{s}$  intermediate markings to guarantee that at most one robot enters any cell between two consecutive synchronizations:

$$\begin{aligned} & \text{Minimize} && \sum_{i=1}^{\bar{s}} \mathbf{1}^T \cdot \boldsymbol{\sigma}_i \cdot (1 + (\bar{s} - i)) \\ & \text{Subject to:} && \mathbf{m}_i = \mathbf{m}_{i-1} + \mathbf{C} \cdot \boldsymbol{\sigma}_i, \quad i = 1, \dots, \bar{s}, \quad (a) \\ & && \mathbf{x} \leq \mathbf{V} \cdot \mathbf{m}_{\bar{s}} \leq \mathbf{N} \cdot \mathbf{x}, \quad (b) \\ & && \mathbf{A}_\varphi \cdot \mathbf{x} \leq \mathbf{b}_\varphi, \quad (c) \\ & && \mathbf{Post} \cdot \boldsymbol{\sigma}_i + \mathbf{m}_{i-1} \leq \mathbf{1}, \quad i = 1, \dots, \bar{s}, \quad (d) \\ & && \mathbf{m}_i \in \mathbb{R}_{\geq 0}^{|\mathcal{P}|}, \quad \boldsymbol{\sigma}_i \in \mathbb{R}_{\geq 0}^{|\mathcal{T}|}, \quad i = 1, \dots, \bar{s}. \quad (e) \\ & && \mathbf{x} \in \{0, 1\}^{|\mathcal{Y}|} \end{aligned} \quad (8)$$

Here,  $\mathbf{m}_i$  and  $\boldsymbol{\sigma}_i$  denote the markings and firing vectors at each synchronization step, while  $\mathbf{x}$  enforces the Boolean specification at the final state. By Theorem 4, the constraint matrix of (8) (excluding the Boolean rows) is TU; hence, apart from the binary variables in  $\mathbf{x}$ , MILP (8) yields integer solutions for  $\mathbf{m}_i$  and  $\boldsymbol{\sigma}_i$ . If the problem is infeasible,  $\bar{s}$  can be incremented and the problem re-solved. In practice, we observed that only a few additional synchronizations were sufficient to restore feasibility.

Algorithm 1 describes the two-stage procedure. First, the relaxed LP version of problem (5) is solved to detect infeasibility early and estimate the minimal congestion level  $s^*$ . If this yields a valid integer solution, the process stops. Otherwise, a refinement stage is applied, where a MILP with  $\bar{s}$  intermediate synchronizations is solved until a collision-free plan consistent with the Boolean specification is obtained. This two-stage procedure ensures both completeness and soundness. Whenever a

---

**Algorithm 1: Two-Stage Planner with Boolean Specs**


---

**Input:** RMPN  $\Sigma_{\mathcal{N}} = \langle P, T, \text{Pre}, \text{Post} \rangle$ , initial marking  $\mathbf{m}_0$ ; labeling matrix  $\mathbf{V}$ ; Boolean constraints  $\langle \mathbf{A}_\varphi, \mathbf{b}_\varphi \rangle$ ; big constants  $M, N$ .

**Output:** Collision-free plan: integer  $\{\mathbf{m}_i, \boldsymbol{\sigma}_i\}_{i=1}^{\bar{s}}$  and binary  $\mathbf{x}$ ; or *infeasible*.

- 1 **Stage I: Solve (5)-LP (all variables relaxed)**
- 2 Solve (5)-LP with decision variables  $(\mathbf{m}, \boldsymbol{\sigma}, \mathbf{x}, s)$
- 3 **if LP infeasible then**
- 4 | **return infeasible**
- 5 **end**
- 6 Let  $(\mathbf{m}^*, \boldsymbol{\sigma}^*, \mathbf{x}^*, s^*)$  be the optimal solution of (5)-LP
- 7 **if**  $s^* = 1$  **and**  $\mathbf{x}^* \in \{0, 1\}^{|\mathcal{Y}|}$  **then**
- 8 | // TU implies  $\mathbf{m}^*, \boldsymbol{\sigma}^*$  are integer
- 9 | **return**  $\bar{s} = 1, \mathbf{m}_1 = \mathbf{m}^*, \boldsymbol{\sigma}_1 = \boldsymbol{\sigma}^*, \mathbf{x} = \mathbf{x}^*$
- 10 **else**
- 11 |  $\bar{s} \leftarrow \lceil s^* \rceil$  // min. # synchronizations
- 12 **end**
- 13 **Stage II: Collision-free refinement with intermediate markings**
- 14 **for**  $k := \bar{s}$  **to**  $n_R$  **do**
- 15 | Solve (8)-MILP with variables  $\{\mathbf{m}_i, \boldsymbol{\sigma}_i\}_{i=1}^k \in \mathbb{R}$ ,  $\mathbf{x} \in \{0, 1\}^{|\mathcal{Y}|}$
- 16 | **if (8)-MILP feasible then**
- 17 | // By TU (Thm. 4),  $\mathbf{m}_i, \boldsymbol{\sigma}_i$  are integer
- 18 | **return**  $\bar{s} = k, \{\mathbf{m}_i, \boldsymbol{\sigma}_i\}_{i=1}^k, \mathbf{x}$
- 19 | **end**
- 20 **end**
- 21 **return infeasible**

---

feasible plan exists, the algorithm will find one, and this plan will satisfy the Boolean-based goal.

*Solution complexity:* We propose an effective strategy to deal with the NP-hard nature of the ILP problems since the LP relaxation of an ILP problem is solvable in polynomial time using well-established algorithms, such as the simplex method [42]. The number of unknown variables in Stage I, i.e., (5)-LP, is equal to  $|\mathcal{P}| + |\mathcal{T}| + |\mathcal{Y}| + 1$ , while the number of constraints is  $2 \cdot |\mathcal{P}| + 2 \cdot |\mathcal{Y}| + n_R$ . In Stage II, the size of the (8)-MILP depends on the number of required intermediary markings,  $\bar{s}$ . Here we are dealing with  $\bar{s} \cdot (|\mathcal{P}| + |\mathcal{T}|) + |\mathcal{Y}|$  variables and  $2 \cdot \bar{s} \cdot |\mathcal{P}| + 2 \cdot |\mathcal{Y}| + n_R$  constraints.

*Limitations:* One of the limitations of the method proposed is the interpretation of the Boolean goal which indicates the position of the robots in their final state and not along paths. Moreover, narrow corridors may lead to an increased number of synchronizations, which will slow down the execution as increased coordination will be required. Another limitation arises from the potentially large number of binary variables of vector  $\mathbf{x}$ , corresponding to a high number of regions of interest. This can increase the computational load while solving the MILP formulation in the second stage of the method, but despite these constraints, the algorithm remains highly efficient for a wide range of practical scenarios.

## VII. SIMULATIONS

This section presents simulation results across several scenarios, demonstrating both the efficiency and scalability of the proposed path-planning algorithm. In all exper-

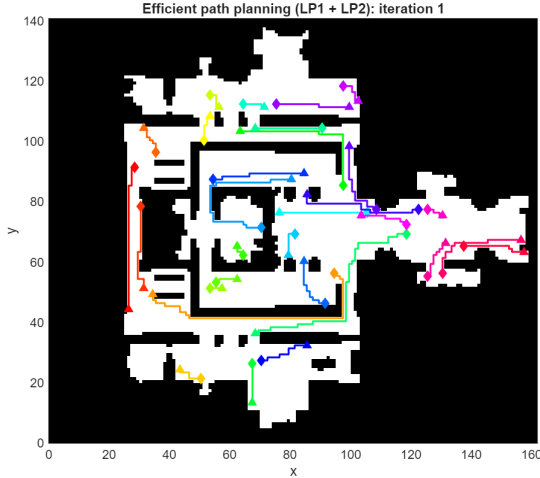


Fig. 2: Example of the *ht\_chantry* benchmark environment used for TAPF simulations. Black pixels denote obstacles, while colored markers represent robots and their assigned goal regions for a trial involving 30 robots. Each free pixel corresponds to a place in the underlying RMPN model.

iments, the regions of interest and the initial robot positions are randomly generated. The simulations were executed on a workstation equipped with an AMD Ryzen 9 9950X 16 CPU and 64 GB of RAM. The MATLAB implementation, available at [https://github.com/IoanaHustiu/efficient\\_TAPF\\_for\\_Boolean\\_specifications.git](https://github.com/IoanaHustiu/efficient_TAPF_for_Boolean_specifications.git), employs the *intlinprog* solver for efficient handling of the optimization constraints.

#### A. Task-Assignment and Path Finding (TAPF) problem

We evaluate the proposed algorithm on the *ht\_chantry* benchmark map from [43]. A pixel-level abstraction is adopted, where *each free pixel corresponds to a place* in the RMPN and transitions represent 4-neighborhood adjacency. The original image has a resolution of  $141 \times 162$  pixels; after removing obstacles (black pixels in Fig. 2, which illustrates a trial with 30 robots), the environment comprises 7,461 free pixels (places) and 27,926 transitions (adjacency arcs). The complete MATLAB implementation is publicly available as script `main_TAPF_chantry.m`.

For each team size, 20 random start–goal configurations were generated from the benchmark map, and the planner jointly optimized task assignment and collision-free paths minimizing total travel distance. We apply Algorithm 1 in a TAPF special case where  $\mathbf{x} = \mathbf{1}$  (a conjunctive global goal over  $n_R$  disjoint goal regions). Thus,  $\mathbf{x}$  can be omitted from the optimization.

- **Stage I:** Solve LP (6); if the resulting trajectories are non-intersecting (i.e.,  $s^* = 1$ ), the process stops.
- **Stage II (if needed):** If intersections occur, solve LP (7), a particular case of MILP (8) with  $\mathbf{x} = \mathbf{1}$ , introducing intermediate markings (synchronizations) to ensure collision-free motion.

Table I summarizes, for each  $n_R$ : (i) *runtimeLP* = runtime of our approach (LP (6) plus, when necessary, LP (7)); (ii) *runtimeILP* = runtime when solving (6) and (7) as *integer*

TABLE I  
TAPF PROBLEM: MEAN VALUES FOR PROPOSED ALGORITHM VS. ILP FORMULATION

$n_R$	runtime (s) ((6) + (7))		cost	synchronizations $\bar{s}$			SR %
	ours (LPs)	ILPs		mean	min	max	
10	0.39	0.44	450.7	1.00	1	1	100
50	1.40	2.37	1329.1	1.40	1	2	100
100	4.75	5.85	2029.3	2.00	1	3	100
250	6.30	8.47	3003.0	2.65	2	5	100
500	9.98	15.83	4413.2	3.52	2	5	85
750	12.77	20.83	5320.5	4.06	2	5	80
1000	13.15	31.87	5794.3	4.50	4	5	50
1250	12.50	20.48	6300.1	4.77	4	5	45
1500	13.08	23.49	6462.5	5.00	5	5	10
1750	10.34	38.61	6724.5	5.00	5	5	10
2000	3.83	37.99	5837.0	4.50	4	5	10
2250	3.52	22.37	7009.0	5.00	5	5	5
2500	–	–	–	–	–	–	0

programs (baseline needed in absence of the results of this paper); (iii)  $cost = \sum_{i=1}^s \mathbf{1}^\top \cdot \boldsymbol{\sigma}_i$  (total number of moves); (iv)  $\bar{s}_{\text{mean}}, \bar{s}_{\text{min}}, \bar{s}_{\text{max}}$  = statistics of the required synchronizations; and (v)  $SR_{\text{percent}}$  = success rate (%). Dividing  $cost$  by  $n_R$  yields the *average path length per robot*, which grows moderately with  $n_R$  as expected.

The main limitation arises from memory usage when multiple synchronizations are required, since the number of variables in LP (7) grows proportionally to  $\bar{s}(|P| + |T|)$ . When  $\bar{s} > 5$ , the constraint matrix may exceed available memory, explaining the observed drop in success rate. In practice, this issue can be mitigated by solving a simplified MILP version with  $s$  as the only integer variable—allowing minor local adjustments for collisions—or by coarsening the map resolution, which reduces the number of places and transitions and keeps the problem tractable for larger teams.

#### B. Boolean-Based Specifications

In this set of experiments, we evaluate the performance of the proposed method when the global task is expressed as a Boolean formula containing multiple disjunctions per term. We consider a fixed team of 100 robots operating in the *warehouse* environment (Fig. 3), which consists of narrow corridors of unit width, allowing only one robot to traverse a corridor at a time. The warehouse layout includes 21 entrances to the shelf corridors, each permitting the passage of a single robot simultaneously. Consequently, the number of intermediate markings required for synchronization is given by the ceiling of the ratio between the number of robots and the number of available corridor entrances, i.e.,  $\lceil n_R/21 \rceil$ . The robots are initially placed randomly on the left side of the map and must reach a set of target regions located in the central area of the warehouse, thereby fulfilling the Boolean goal.

The Boolean specification is generated as a conjunction of  $n_R$  terms, where each term is a disjunction of a randomly chosen number of destination regions:

$$\varphi = (y_1^1 \vee \dots \vee y_{k_1}^1) \wedge (y_1^2 \vee \dots \vee y_{k_2}^2) \wedge \dots \wedge (y_1^{n_R} \vee \dots \vee y_{k_{n_R}}^{n_R}),$$

with each  $k_i$  randomly selected such that  $1 \leq k_i \leq n_P$ . The parameter  $n_P$  is varied between 1 and 10, where  $n_P = 1$  corresponds to the TAPF case (each robot having a single destination). For each configuration, 20 independent trials are

TABLE II  
 BOOLEAN-BASED SPECIFICATION: MEAN VALUES FOR 100  
 ROBOTS IN THE WAREHOUSE ENVIRONMENT.

$n_P$	runtimeMILP	runtimeILP	cost	$\bar{s}$	SR(%)
1	19.35	57.51	6911.1	5	100
2	12.38	48.24	6050.4	5	100
3	13.22	55.93	5477.6	5	100
4	14.96	48.04	5068.9	5	100
5	14.59	51.3	4775.9	5	100
6	16.01	48.31	4562	5	100
7	14.74	46.63	4255.4	5	100
8	15.38	50.97	4229.7	5	100
9	13.71	45.73	3977.6	5	100
10	15.45	50.75	3856.3	5	100

performed, with both the initial positions and goal regions generated randomly in each trial.

Table II reports the mean values over the experiments for both our MILP-based approach and the ILP formulation. The results show that the computational time remains nearly constant as  $n_P$  increases. This behavior indicates that the problem complexity is primarily determined by the number of intermediate markings ( $\bar{s}$ ) required for synchronization, which, as explained earlier, remains constant in this setup, rather than by the number of disjunctions in the formula. Although adding disjunctions increases the number of possible choices for each robot, the overall computational effort of solving MILP (5) and MILP (8) remains stable as long as  $\bar{s}$  does not change.

It should be noted that, in this case, the presence of a Boolean formula introduces binary decision variables  $\mathbf{x}$  into the optimization, corresponding to the possible destinations for the robots. Consequently, the problem becomes a MILP, where the number of binary variables is equal to the number of destination regions included in the Boolean specification.

Additional experiments, including large-scale evaluations and various strategies for rounding the assignment vector  $\mathbf{x}$  in the MILP formulation (8), are reported in [44], where several LP-based rounding techniques are compared in terms of runtime and solution quality across diverse robotic scenarios. These results further validate the efficiency and robustness of the proposed Petri-net-based formulation for solving complex Boolean-goal planning problems.

### C. Comparative Evaluation with MAPF Baselines

To contextualize our contributions, we evaluated the proposed method on four standard MAPF benchmarks from [43]: *room-32-32-4* ( $32 \times 32$ , 682 states), *random-32-32-20* ( $32 \times 32$ , 819 states), *den312d* ( $65 \times 81$ , 2445 states), and *ht\_chantry* ( $162 \times 141$ , 7461 free cells). These maps are widely used to assess scalability in MAPF research, particularly for Conflict-Based Search (CBS) [20] and Priority-Based Search (PBS) [21], [45], yet no existing TAPF approaches have been tested on such large instances.

For each map, 25 random scenarios were generated with the number of robots scaled to roughly half of the available cells, ensuring a unit cell capacity (one robot per cell). Problem (7) was solved using its LP relaxation, with runtime thresholds of 30 s for the smaller maps and 60 s for the larger ones. Figure 4 reports the mean, minimum, and maximum runtimes versus

team size, along with the corresponding number of decision variables.

Across all benchmarks, our method achieved a 100% success rate and near-linear growth in runtime, demonstrating strong computational scalability. Compared with classical MAPF baselines, it remains competitive or faster: Enhanced and Explicit Estimation CBS [46] show rapid performance degradation beyond 100 agents, while the MCP algorithm [45] maintains full success up to 3000 robots but under less expressive formulations. Similarly, MAPF-LNS2 [23] requires roughly an order of magnitude longer runtimes on the same maps. Recent large-scale studies on *ht\_chantry* [47]–[51] reach 1000 robots with specialized heuristics; in contrast, our Petri-net-based approach attains comparable scalability while additionally handling Boolean goal specifications and offering formal guarantees through total unimodularity.

Overall, the proposed formulation bridges the gap between optimization-based TAPF and heuristic MAPF solvers, combining the tractability of LP relaxations with the expressiveness of logical task modeling. It thus provides a unified and scalable framework for large-team coordination where both optimality and logical correctness are required.

## VIII. CONCLUSIONS

This paper is presenting a novel approach for obtaining efficiently collision-free path planning together with task allocation in the context of large teams of mobile robots that have the goal to fulfill a Boolean-based specification. Our primary contribution is to uncover and demonstrate the unique structural properties of the formulated optimization problem - the total unimodularity of the constraint matrix - which is permitting us to avoid solving the classical ILP formulation and use its MILP and LP relaxations. Moreover, the achieved results through the theoretical component are supported by multiple performed simulations with a balance between efficiency and accuracy, making the approach highly effective for applications with teams of up to 2000 robots. Furthermore, the method is guaranteeing optimality even when the collision avoidance is necessary, even though the problem formulation requires introducing new constraints. Future work is aiming to reduce the limitation regarding the expressivity of the global task, first by managing visiting regions along paths and next by employing Temporal Logics such as LTL.

## REFERENCES

- [1] N. Mathew, S. L. Smith, and S. L. Waslander, "Planning paths for package delivery in heterogeneous multirobot teams," *IEEE Trans. on Autom. Science and Eng.*, vol. 12, no. 4, pp. 1298–1308, 2015.
- [2] M. Debord, W. Hönig, and N. Ayanian, "Trajectory planning for heterogeneous robot teams," in *2018 IEEE/RSJ Int. Conf. on Intell. Robot. and Syst. (IROS)*, 2018, pp. 7924–7931.
- [3] D. R. Robinson, R. T. Mar, K. Estabridis, and G. Hoyer, "An efficient algorithm for optimal trajectory generation for heterogeneous multi-agent systems in non-convex environments," *IEEE Robot. and Autom. Lett.*, vol. 3, no. 2, pp. 1215–1222, 2018.
- [4] J. Yu and S. M. LaValle, "Optimal multirobot path planning on graphs: complete algorithms and effective heuristics," *IEEE Trans. on Robot.*, vol. 32, no. 5, pp. 1163–1177, 2016.
- [5] S. Ardizzoni, L. Consolini, M. Locatelli, and I. Saccani, "Constrained motion planning and multi-agent path finding on directed graphs," *Automatica*, vol. 165, p. 111593, 2024.

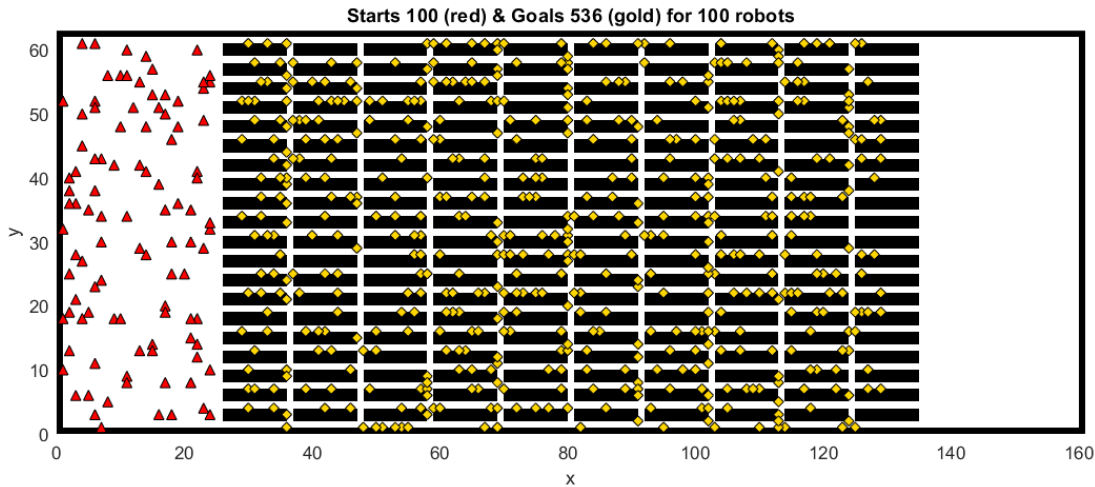


Fig. 3: Example of warehouse environment used in Boolean-based experiments. Robots start on the left side and must reach central regions that satisfy a randomly generated Boolean formula. Each corridor can host at most one robot at a time.

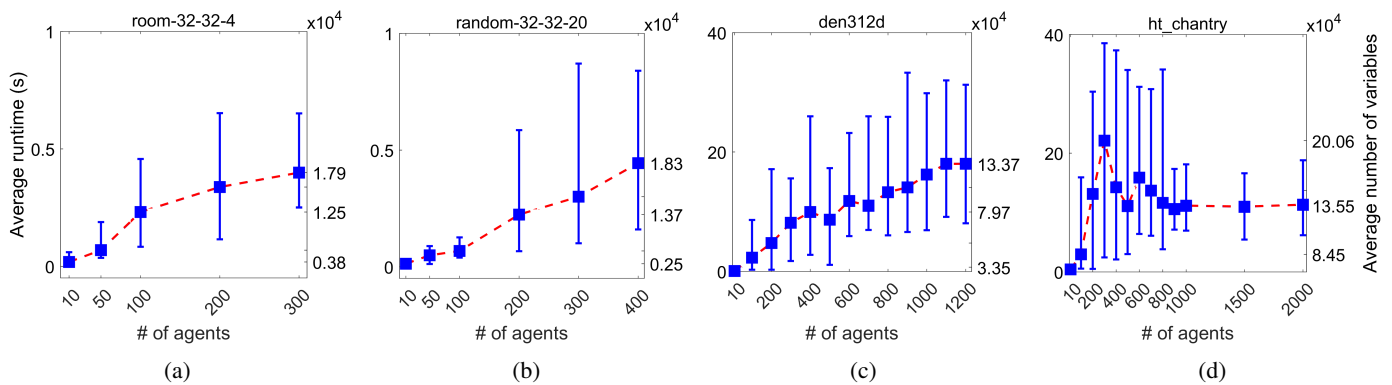


Fig. 4: Runtime measured in seconds for *room-32-32-4*, *random-32-32-20*, *den312d*, and *ht\_chantry* maps.

- [6] B. D. Song, J. Kim, and J. R. Morrison, “Rolling horizon path planning of an autonomous system of UAVs for persistent cooperative service: MILP formulation and efficient heuristics,” *J. of Intell. & Robot. Syst.*, vol. 84, pp. 241–258, 2016.
- [7] P. Ghassemi and S. Chowdhury, “Multi-robot task allocation in disaster response: addressing dynamic tasks with deadlines and robots with range and payload constraints,” *Robot. and Autonomous Syst.*, vol. 147, p. 103905, 2022.
- [8] T. Schouwenaars, B. De Moor, E. Feron, and J. How, “Mixed integer programming for multi-vehicle path planning,” in *2001 European control Conf. (ECC)*. IEEE, 2001, pp. 2603–2608.
- [9] A. Richards and J. P. How, “Aircraft trajectory planning with collision avoidance using mixed integer linear programming,” in *Proc. of the 2002 American Control Conf. (IEEE Cat. No. CH37301)*, vol. 3. IEEE, 2002, pp. 1936–1941.
- [10] K. Kalyanam, S. Manyam, A. Von Moll, D. Casbeer, and M. Pachter, “Scalable and exact MILP methods for UAV persistent visitation problem,” in *2018 IEEE Conf. on Control Technology and Applications (CCTA)*, 2018, pp. 337–342.
- [11] L. Alfandari, I. Ljubić, and M. D. M. da Silva, “A tailored Benders decomposition approach for last-mile delivery with autonomous robots,” *European J. of Operational Res.*, vol. 299, no. 2, pp. 510–525, 2022.
- [12] C. Mahulea, M. Kloetzer, and J.-J. Lesage, “Multi-robot path planning with Boolean specifications and collision avoidance,” *IFAC-PapersOnLine*, vol. 53, no. 4, pp. 101–108, 2020.
- [13] P. Lv, G. Luo, Z. Ma, S. Li, and X. Yin, “Optimal multi-robot path planning for cyclic tasks using Petri nets,” *Control Eng. Practice*, vol. 138, p. 105600, 2023.
- [14] S. Hustiu, C. Mahulea, M. Kloetzer, and J.-J. Lesage, “On multi-robot path planning based on Petri net models and LTL specifications,” *IEEE Trans. on Autom. Control*, vol. 69, no. 9, pp. 6373–6380, 2024.
- [15] V. A. Ziparo, L. Iocchi, P. U. Lima, D. Nardi, and P. F. Palamara, “Petri net plans: a framework for collaboration and coordination in multi-robot systems,” *Autonomous Agents and Multi-Agent Syst.*, vol. 23, pp. 344–383, 2011.
- [16] B. Lacerda and P. U. Lima, “Petri net based multi-robot task coordination from temporal logic specifications,” *Robot. and Autonomous Syst.*, vol. 122, p. 103289, 2019.
- [17] C. Mahulea and M. Kloetzer, “Robot planning based on Boolean specifications using Petri net models,” *IEEE Trans. on Autom. Control*, vol. 63, no. 7, pp. 2218–2225, 2018.
- [18] R. Abolpour and C. Mahulea, “Optimizing path-planning solutions obtained by using Petri nets models,” *IFAC-PapersOnLine*, vol. 58, no. 1, pp. 240–245, 2024.
- [19] H. Ma and S. Koenig, “Optimal target assignment and path finding for teams of agents,” *arXiv preprint arXiv:1612.05693*, 2016.
- [20] G. Sharon, R. Stern, A. Felner, and N. R. Sturtevant, “Conflict-based search for optimal multi-agent pathfinding,” *Artificial Intell.*, vol. 219, pp. 40–66, 2015.
- [21] H. Ma, D. Harabor, P. J. Stuckey, J. Li, and S. Koenig, “Searching with consistent prioritization for multi-agent path finding,” in *Proc. of the AAAI Conf. on Artificial Intell.*, vol. 33, no. 01, 2019, pp. 7643–7650.
- [22] Z. Liu, H. Wei, H. Wang, H. Li, and H. Wang, “Integrated task allocation and path coordination for large-scale robot networks with uncertainties,” *IEEE Trans. on Autom. Science and Eng.*, vol. 19, no. 4, pp. 2750–2761, 2021.
- [23] J. Li, Z. Chen, D. Harabor, P. J. Stuckey, and S. Koenig, “MAPF-LNS2: Fast repairing for multi-agent path finding via large neighborhood search,” in *Proc. of the AAAI Conf. on Artificial Intell.*, vol. 36, no. 9, 2022, pp. 10256–10265.
- [24] W. Hönig, S. Kiesel, A. Tinka, J. Durham, and N. Ayanian, “Conflict-

- based search with optimal task assignment,” in *Proc. of the Int. Joint Conf. on Autonomous Agents and Multiagent Syst.*, 2018.
- [25] C. Henkel, J. Abbenseth, and M. Toussaint, “An optimal algorithm to solve the combined task allocation and path finding problem,” in *2019 IEEE/RSJ Int. Conf. on Intell. Robot. and Syst. (IROS)*. IEEE, 2019, pp. 4140–4146.
- [26] H.-L. Choi, L. Brunet, and J. P. How, “Consensus-based decentralized auctions for robust task allocation,” *IEEE Trans. on Robot.*, vol. 25, no. 4, pp. 912–926, 2009.
- [27] D.-H. Lee, S. A. Zaheer, and J.-H. Kim, “A resource-oriented, decentralized auction algorithm for multirobot task allocation,” *IEEE Trans. on Autom. Science and Eng.*, vol. 12, no. 4, pp. 1469–1481, 2014.
- [28] S. Chen, M. Wang, and W. Song, “Hierarchical learning with heuristic guidance for multi-task assignment and distributed planning in interactive scenarios,” *IEEE Trans. on Intell. Vehicles*, 2024.
- [29] X. Xu, Q. Yin, Z. Quan, B. Ju, and J. Miao, “Heuristic-based task assignment and multi-agent path planning for automatic warehouses,” in *2023 China Autom. Congress (CAC)*. IEEE, 2023, pp. 1490–1495.
- [30] Z. Chen, C. Chen, Y. Ni, and J. Wang, “Heuristically guided compilation for task assignment and path finding,” in *2025 IEEE Int. Conf. on Robot. and Autom. (ICRA)*. IEEE, 2025, pp. 7741–7747.
- [31] K. Brown, O. Peltzer, M. A. Sehr, M. Schwager, and M. J. Kochenderfer, “Optimal sequential task assignment and path finding for multi-agent robotic assembly planning,” in *2020 IEEE Int. Conf. on Robot. and Autom. (ICRA)*. IEEE, 2020, pp. 441–447.
- [32] P. Arias-Melia, J. Liu, and R. Mandania, “The vehicle sharing and task allocation problem: Milp formulation and a heuristic solution approach,” *Computers & Operations Research*, vol. 147, p. 105929, 2022.
- [33] G. Sartoretti, J. Kerr, Y. Shi, G. Wagner, T. S. Kumar, S. Koenig, and H. Choset, “Primal: Pathfinding via reinforcement and imitation multi-agent learning,” *IEEE Robot. and Autom. Lett.*, vol. 4, no. 3, pp. 2378–2385, 2019.
- [34] W. Li, H. Chen, B. Jin, W. Tan, H. Zha, and X. Wang, “Multi-agent path finding with prioritized communication learning,” in *2022 Int. Conf. on Robot. and Autom. (ICRA)*. IEEE, 2022, pp. 10 695–10 701.
- [35] A. Skrynnik, A. Andreychuk, K. Yakovlev, and A. I. Panov, “When to switch: planning and learning for partially observable multi-agent pathfinding,” *IEEE Trans. on Neural Networks and Learning Syst.*, 2023.
- [36] J. Xie, Y. Zhang, H. Yang, Q. Ouyang, F. Dong, X. Guo, S. Jin, and D. Shi, “Crowd perception communication-based multi-agent path finding with imitation learning,” *IEEE Robot. and Autom. Lett.*, 2024.
- [37] H. Zhang, J. Luo, X. Lin, K. Tan, and C. Pan, “Dispatching and path planning of automated guided vehicles based on petri nets and deep reinforcement learning,” in *2021 IEEE Int. Conf. on Networking, Sensing and Control (ICNSC)*, vol. 1. IEEE, 2021, pp. 1–6.
- [38] S. M. LaValle, *Planning algorithms*. Cambridge University Press, 2006, available at <https://lavalle.pl/planning/>.
- [39] C. Mahulea, M. Kloetzer, and R. González, *Path planning of cooperative mobile robots using discrete event models*. Wiley-IEEE Press, 2020.
- [40] M. Kloetzer and C. Mahulea, “Path planning for robotic teams based on LTL specifications and Petri net models,” *Discrete Event Dynamic Syst.*, vol. 30, no. 1, pp. 55–79, 2020.
- [41] A. Schrijver, *Theory of linear and integer programming*. Wiley & Sons Ltd, 1998.
- [42] D. A. Spielman and S.-H. Teng, “Smoothed analysis of algorithms: why the simplex algorithm usually takes polynomial time,” *J. of the ACM (JACM)*, vol. 51, no. 3, pp. 385–463, 2004.
- [43] R. Stern, N. Sturtevant, A. Felner, S. Koenig, H. Ma, T. Walker, J. Li, D. Atzmon, L. Cohen, T. Kumar *et al.*, “Multi-agent pathfinding: definitions, variants, and benchmarks,” in *Proc. of the Int. Symposium on Combinatorial Search*, vol. 10, no. 1, 2019, pp. 151–158.
- [44] I. Hustiu, M. Kloetzer, and C. Mahulea, “Motion Planning for Mobile Robots Through Iterative Task Allocation,” in *2025 IEEE Conference on Control Technology and Applications (CCTA)*, 2025, pp. 780–785.
- [45] P. Friedrich, Y. Zhang, M. Curry, L. Dierks, S. McAleer, J. Li, T. Sandholm, and S. Seuken, “Scalable mechanism design for multi-agent path finding,” *arXiv preprint arXiv:2401.17044*, 2024.
- [46] J. Li, W. Ruml, and S. Koenig, “Eecbs: A bounded-suboptimal search for multi-agent path finding,” in *Proc. of the AAAI Conf. on Artificial Intell.*, vol. 35, no. 14, 2021, pp. 12 353–12 362.
- [47] Z. Ren, A. Nandy, S. Rathinam, and H. Choset, “DMS\*: Towards minimizing makespan for multi-agent combinatorial path finding,” *IEEE Robot. and Autom. Lett.*, 2024.
- [48] A. Pertzovsky, R. Zivan, and R. Stern, “Adapting distributed constraint optimization for modeling and solving distributed multi-agent pathfinding,” Available at SSRN 5013125, 2025.

- [49] R. Veerapaneni, M. S. Saleem, J. Li, and M. Likhachev, “Windowed MAPF with completeness guarantees,” in *Proc. of the AAAI Conf. on Artificial Intell.*, vol. 39, no. 22, 2025, pp. 23 323–23 332.
- [50] Z. A. Ali and K. Yakovlev, “Improved anonymous multi-agent path finding algorithm,” in *Proc. of the AAAI Conf. on Artificial Intell.*, vol. 38, no. 16, 2024, pp. 17 291–17 298.
- [51] N. Gandotra, R. Veerapaneni, M. S. Saleem, D. Harabor, J. Li, and M. Likhachev, “Anytime single-step MAPF planning with anytime PIBT,” *arXiv preprint arXiv:2504.07841*, 2025.



**Ioana Hustiu** received the B.S. in 2020 and the M.Sc. degree in 2022 in automatic control and applied informatics from the Technical University of Iasi, Romania, where she is a Ph.D. student.

Her research interests include task allocation and path planning in context of distributing high-level specification for multi-robot systems using discrete event systems.



**Roozbeh Abolpour** received the B.Sc. degrees, one in electrical engineering control and another in computer engineering from Shiraz University, Shiraz, Iran, in 2012 and 2014, respectively, the M.Sc. degree in electrical engineering with a concentration in control from the Sharif University of Technology, Tehran, Iran, in 2014, and the Ph.D. degree in electrical engineering, specializing in control, from Shiraz University, Shiraz, Iran, in 2020.

He is currently a Postdoctoral Researcher with the Energy Information Networks and Systems Group at the Technical University of Darmstadt, Darmstadt, Germany. His research interests include control systems, data-driven model predictive control, quadratically constrained quadratic programming, and the optimal power flow problem.



**Marius Kloetzer** received the B.S. and M.Sc. degrees in computer science from the Technical University of Iasi, Romania, in 2002 and 2003, respectively, and the Ph.D. degree in systems engineering from Boston University, MA, USA, in 2008. He is currently a Full Professor with the Technical University of Iasi, Romania. His research interests include formal tools for discrete event systems with applications in motion planning for mobile robots.

Marius Kloetzer was a visiting researcher at Ghent University, Belgium, and at the University of Zaragoza, Spain. He has been Organizing Committee chair at ICSTCC’2017 and Work-in-Progress co-chair at ETFA’2019.



**Cristian Mahulea** received his B.S. and M.Sc. degrees in control engineering from the Technical University of Iasi, Romania, in 2001 and 2002, respectively, and his Ph.D. in systems engineering from the University of Zaragoza, Spain, in 2007. Currently, he is a Full Professor at the University of Zaragoza, where he chaired the Department of Computer Science and Systems Engineering from 2020 to 2024. He has also served as a visiting professor at the University of Cagliari, Italy, and has been a visiting researcher at the University of

Sheffield (UK), Boston University (USA), University of Cagliari (Italy), and ENS Paris-Saclay (France).

He is currently an Associate Editor for IEEE Transactions on Automatic Control (TAC), the International Journal of Robotics Research (IJRR), and Discrete Event Dynamic Systems: Theory and Applications (JDES). He was the General Chair of ETFA 2019 and was AE for IEEE Transactions on Automation Science and Engineering (TASE) and IEEE Control Systems Letters (L-CSS).

APPENDIX A  
PROOF OF THEOREM 3

Suppose  $\mathbf{A} = \begin{bmatrix} \mathbf{C} \\ \mathbf{Post} \end{bmatrix} \in \mathbb{R}^{2|P| \times |T|}$  and  $\mathbf{A}_e$  is an arbitrary  $k^{\text{th}}$  dimensional square sub-matrix of  $\mathbf{A}$  which is obtained through selecting  $R$  rows and  $C$  columns of  $\mathbf{A}$  such that  $R$  and  $C$  are arbitrary subsets of  $\{1, \dots, 2|P|\}$  and  $\{1, \dots, |T|\}$ .

Since each column of matrix  $\mathbf{C}$  contains one and only one entry 1 and  $-1$ , we can define  $r_+(c)$  and  $r_-(c)$  to be the row indices of 1 and  $-1$  entries in the  $c^{\text{th}}$  column of  $\mathbf{C}$  for each  $c \in C$ .

Let sets  $R_1 \subset R$  and  $R_2 \subset R$  be defined as follows:

$$\begin{aligned} R_{1_1} &= \{r \in R \mid r \leq |P|\} \\ R_{1_2} &= \{r \in R \mid r > |P| \wedge \\ &(\forall c \in C : r - |P| \neq r_+(c) \vee r_+(c) \notin R)\} \\ R_1 &= R_{1_1} \cup R_{1_2} \\ R_2 &= R - R_1 \end{aligned} \quad (9)$$

Now, suppose  $c \in C$  is arbitrarily selected and consider the following cases, which cover all possible situations.

**Case 1.** Assume  $r_+(c) \in R_1$ . If there exists  $r \in R_{1_2}$  such that  $r - |P| = r_+(c)$ , then we must have  $r_+(c) \notin R$  based on (9) which openly contradicts  $r_+(c) \in R_1 \subset R$ . Thus, it can be successively concluded that  $C_{r-|P|,c} \in \{-1, 0\}$ ,  $Post_{r-|P|,c} = 0$ , and  $A_{r,c} = 0$  for all  $r \in R_{1_2}$ .

Using (9), the fact that  $c^{\text{th}}$  column of matrix  $\mathbf{C}$  has one and only one element  $+1$  and  $-1$ , and the assumption of this case, we have:

$$\begin{aligned} \sum_{r \in R_1} A_{r,c} &= \sum_{r \in R_{1_1}} A_{r,c} + \sum_{r \in R_{1_2}} A_{r,c} = \sum_{r \in R_1} C_{r,c} = \\ &\left( \sum_{r \in R_1 - \{r_+(c)\}} C_{r,c} \right) + C_{r_+(c),c} = \\ &\left( \sum_{r \in R_1 - \{r_+(c)\}} C_{r,c} \right) + 1 \in \{0, 1\} \end{aligned} \quad (10)$$

$$\sum_{r \in R_2} A_{r,c} = \sum_{r \in R_2} Post_{r-|P|,c} \in \{0, 1\} \quad (11)$$

$$\sum_{r \in R_1} A_{r,c} - \sum_{r \in R_2} A_{r,c} \in \{-1, 0, 1\} \quad (12)$$

**Case 2.** Assume  $r_+(c) \notin R_1$ . If there is  $r \in R_2$  such that  $r - |P| = r_+(c)$ , then we must have  $r_+(c) \in R$  and  $r_+(c) \in R_1$  (note that  $r \notin R_{1_2}$  since it has been supposed to be within  $R_2$ ) owing to (9) which opposes the assumption of this case. Thereby, we successively have  $C_{r-|P|,c} \in \{0, -1\}$ ,  $Post_{r-|P|,c} = 0$ , and  $A_{r,c} = Post_{r-|P|,c} = 0$  for all  $r \in R_2$ . Added to this, it can be simply concluded that  $\sum_{r \in R_{1_1}} C_{r,c} \in \{-1, 0\}$  since  $r_+(c) \notin R_{1_1}$ . These facts directly lead to the next relations:

$$\sum_{r \in R_1} A_{r,c} = \sum_{r \in R_{1_1}} C_{r,c} + \sum_{r \in R_{1_2}} Post_{r-|P|,c} \in \{-1, 0, 1\} \quad (13)$$

$$\sum_{r \in R_2} A_{r,c} = \sum_{r \in R_2} Post_{r-|P|,c} = \sum_{r \in R_2} Post_{r-|P|,c} = 0 \quad (14)$$

Therefore, we have  $\sum_{r \in R_1} A_{r,c} - \sum_{r \in R_2} A_{r,c} \in \{-1, 0, +1\}$  for all  $c \in \{1, \dots, n\}$  in both cases that complete the proof based on Ghouila-Houri's characterization. Thus, the matrix  $\begin{bmatrix} \mathbf{C} \\ \mathbf{Post} \end{bmatrix}$  is totally unimodular.